Energy & Buildings 278 (2023) 112621

Contents lists available at ScienceDirect

Energy & Buildings

journal homepage: www.elsevier.com/locate/enb

Performance analysis of a stand-alone thermal energy storage system based on CSM plates filled with phase change material

Hafiz Muhammad Adeel Hassan [a,*], Mads Peter Rudolph Hansen [b], Jonathan Dallaire [c], Martin Anker Boesen Larsen [d], Esther Kieseritzky [e], Joe Alexandersen [a], Christian Veje [c], Ivar Lund [a]

[a] Department of Mechanical and Electrical Engineering, University of Southern Denmark, Campusvej 55, 5230 Odense, Denmark
[b] Danish Technological Institute, Energy and Climate, Gregersensvej 2630 Taastrup, Denmark
[c] Center for Energy Informatics, Mærsk Mckinney Møller Institute, University of Southern Denmark, Campusvej 55, 5230 Odense, Denmark
[d] Exhausto A/S, Odensevej 76, 5550 Langeskov, Denmark
[e] Rubitherm Technologies GmbH, Imhoffweg 6, 12307 Berlin, Germany

ARTICLE INFO

Article history:
Received 16 May 2022
Revised 18 August 2022
Accepted 27 October 2022
Available online 03 November 2022

Keywords:
Phase change material
Thermal energy storage
Building cooling
CSM plate

ABSTRACT

In this study, experimental investigations on a Phase Change Material (PCM) based thermal energy storage system (TES) were carried out. The TES system was designed and tested as a first step of developing a potential TES product which can be integrated with commercially available ventilation system (VEX308) to provide cold intake air for space cooling applications. The system consisted of wedge-shaped air flow regions before and after an array of Compact Storage Module (CSM) plates filled with PCM and arranged vertically with air gaps between the plates. Two design configurations of the TES system were investigated based on air gap size between PCM plates (1.5 mm and 3 mm) in order to compare them for pressure loss through the system and thermal performance of the PCM storage. Investigations were done at two air flow rates of 400 m^3/h and 800 m^3/h which were within the working range of VEX308 for fixed air inlet temperatures of 27 °C and 13 °C for heating and cooling cycles of the PCM storage, respectively. The temperatures ranges were chosen to investigate the application of the TES system during summer season in Denmark. Parameters investigated were: pressure loss through the TES system, pressure distribution from top to bottom in the TES system before and after the PCM stack, temperature distribution in the TES system from top to bottom, and melting and solidification rates of the PCM. Results showed that pressure drop through the system, for both configurations, was well within the desired limits ($< 180Pa$) for a successful integration of the TES system with VEX308. Temperature distribution was relatively fair from top to bottom of the PCM stack indicating an adequate inlet manifold design. The 1.5 mm gap configuration (55 CSM plates and 110 kg PCM) showed faster heating and cooling rates at both flow rates as compared to 3 mm system (50 CSM plates and 100 kg PCM). Both systems showed almost same system efficiency (78.3%) for the utilization of the PCM. The 1.5 mm system provided approximately 8.7% more energy storage potential than the 3 mm system because of the presence of 10 kg of extra PCM.

1. Introduction

The demand of energy in the world is ever increasing due to the increase in world's population which has consequently resulted in escalating energy use in industrial, residential and transport sectors [1].The building sector has a share of almost 40% of total world energy use [2] and according to one study, it is estimated to increase by 48% by the end of year 2040 [3]. Faraj et al. [4] concluded that the major use of energy in buildings (almost 50% to 60%) is by heating, ventilating and air-conditioning (HVAC) systems to maintain comfort conditions for the habitants of buildings. An increase in energy demand also increases greenhouse gas emissions and global warming [5]. Keeping in view the increasing demand of energy in buildings sector, there is an urgent need of implementing new energy efficient designs for the buildings, as well as introducing innovative methods to increase energy efficiency of the buildings.

Abbreviations: CSM, Compact Storage Module; HVAC, Heating Ventilation and Air-Conditioning; LHTES, Latent Heat Thermal Energy Storage; PCM, Phase Change Material; TES, Thermal Energy Storage.

* Corresponding author.
E-mail address: m.adeel16@gmail.com (H.M.A. Hassan).

https://doi.org/10.1016/j.enbuild.2022.112621
0378-7788/

Nomenclature

Nomenclature

$C_{p,air}$	specific heat capacity of air [kJ/kg.K]
$C_{p,casing}$	specific heat capacity of the casing material [kJ/kg.K]
$C_{p,PCM}$	specific heat capacity of the PCM [kJ/kg.K]
$C_{p,rack}$	specific heat capacity of the rack material [kJ/kg.K]
h	latent heat of fusion of the PCM [kJ/kg]
$\dot{m}_{air}$	mass flow rate of air [kg/s]
m_{casing}	mass of the casing [kg]
m_{casing}	total mass of the PCM [kg]
m_{rack}	mass of the rack [kg]
Q_{casing}	energy stored by the system casing [kJ]
$Q_{envir.}$	energy lost to the environment [kJ]
$Q_{gain,PCM}$	energy absorbed by the PCM [kJ]
$Q_{PCM,latent}$	latent heat storage potential [kJ]
$Q_{PCM,sensible}$	sensible heat storage potential [kJ]
$Q_{PCM,th}$	theoretical heat storage potential of the PCM [kJ]
Q_{rack}	energy stored by the rack [kJ]
Q_{system}	energy absorbed by the system [kJ]
T_1	PCM plate surface temperature at location 1 [°C]
T_2	PCM plate surface temperature at location 2 [°C]
T_3	PCM plate surface temperature at location 3 [°C]
$T_{air,in}$	inlet temperature of the air [°C]
$T_{air,out}$	outlet temperature of the air [°C]
T_{final}	final temperature of the system components [°C]
$T_{initial}$	initial temperature of the system components [°C]
t	time [s]

Many techniques are being investigated to lower the use of electricity during the summer season to maintain comfort conditions inside buildings. Some of them are evaporative cooling, soil cooling and ventilation cooling [6–8]. Comprehensive reviews of passive cooling techniques used for building cooling applications have been presented in the research articles of [1,4]. Another technique, called free cooling, utilizes an innovative concept of Latent Heat Thermal Energy Storage (LHTES) in which a dedicated thermal mass (other than the mass of building material) is used to improve the energy efficiency of the building by reducing the cooling load [6,9,10]. The materials used as heat storing medium in TES technique are termed as Phase Change Materials (PCMs) [11]. These materials have received the attention of the scientific community because of the advantage of their high energy storage density and storing the heat energy at almost constant phase transition temperature [12]. There are two main types of PCMs used in building cooling applications: organic PCMs and inorganic PCMs. Both types have their own advantages and disadvantages and find their applications according to specific requirements. Shazim [13] presented an overview of advantages and disadvantages associated with both organic and inorganic PCMs. Organic PCMs have the advantages of availability in wider temperature ranges, being chemically non-reactive, no phase segregation issue, low vapour pressure in liquid state, relatively inexpensive, very small or low supercooling, etc. Their disadvantages include low thermal conductivity values, flammability, not suitable for plastic containers. On the other hand, inorganic PCMs have higher latent heat storage per unit volume, higher thermal conductivity, higher heat of fusion, non-flammable nature, compatibility with plastic containers, etc. But they have the disadvantages of being corrosive to metals, exhibit the phenomenon of supercooling during the solidification process, phase segregation, higher vapour pressure in liquid state and higher volume change [13]. PCM based thermal energy storage works on the principle of storing or releasing thermal energy by changing the phase of the material [14]. During the process of charging the PCM storage, the low temperature cold air is passed through the melted PCM (usually during night time) which removes heat stored in the PCM and the PCM is said to be charged. During this process, the PCM changes phase from liquid to solid. While during the discharging process of the PCM storage, outdoor air at higher temperature than the melting temperature of the PCM is passed through the solid PCM. The PCM is melted by absorbing heat from air and, consequently, the air is cooled down [6,15].

Kumirai et al. [16] performed an experimental study on three types of phase change materials including two organic type and one inorganic type, to evaluate their melting behaviors for different inlet air temperatures and velocities. The PCMs were encapsulated in plates, arranged vertically in an air duct system. They concluded that the cooling power increased with increasing velocities and inlet air temperatures while the average thermal effectiveness decreased at increasing velocities. Zeinelabdein et al. [17] experimentally tested a TES system consisting of stacked PCM plates with variable gap spacing between the plates for building cooling application in hot arid regions. The results showed that the charging time for the PCM storage was reduced by 10–14% by reducing the spacing between the plates. A numerical model was also developed by the authors [18] to study the performance of the PCM storage for a domestic room application. They found out that the TES system was capable of saving approximately 67% building cooling energy load during the summer season as compared to conventional air-conditioning system for selected climate zone. In another work, Saeed et al. [19] studied three different organic PCMs encapsulated in slab-plates numerically and experimentally for their integration with solar air heater. They investigated the effect of air inlet temperature, flow rate and density of PCM on the thermal behavior of the multi-PCM based energy storage with variable slab plate thicknesses. They found that thermal performance of the energy storage was improved by 12% by using multiple-PCM energy storage unit compared to single-PCM energy storage unit for winter season application. Mureil et al. [20] constructed a small scale prototype of an air-PCM heat exchanger to investigate the effect of a range of air inlet temperatures and velocities on melting and solidification rates of phase change material, cooling/heating load and effectiveness of the system for phase transition of the PCM. They found out that the melting and solidification rates were increased by increasing air velocities. The average cooling loads were also increased by increasing velocities at a constant air inlet temperature. For inlet velocity of 0.6 m/s, the effectiveness reached the highest value of 0.38 during discharging and 0.16 during charging of the PCM. Nada et al. [21] conducted an experimental study to look into the potential of cooling fresh air for air-conditioning system using thermal energy storage comprising of PCM plates at different flow rates. They found that the time for melting the PCM was reduced 64% when the air flow rate was increased from 89 L/s to 180 L/s at constant temperature of 34 °C. By keeping the flow rate constant, the melting time was reduced by one-third by increasing inlet temperature from 32 °C to 36 °C. Nekoonam and Roshandel [22] numerically investigated a system of solar collector and a PCM-based cascaded energy storage comprising of three different organic PCMs. They developed a two-dimensional transient thermal model to determine the temperature distribution within the PCM energy storage unit. The most important finding was that PCM charging efficiency was improved by 7% by using multiple- PCM energy storage unit at its optimal configuration. Gohar and Mohammad [23] performed experimental investigation on an active thermal energy storage system (with PCM plates vertically arranged) and studied its performance for winter and summer seasons. They reported that the system provided 10.3% to 40% energy savings for both heating season and 10% to 30% during cooling season for the designed facility in New Zealand. In another study, Chen et al. [24] developed a dynamic computational model to investigate the possibility of integrating phase change material based thermal energy storage system in air conditioned buildings. The case was investigated for a south-facing office room in China. The indoor thermal environment and energy consumption were simulated for the room. They concluded that the role of cooling provided by the PCM based thermal energy storage increases by increasing the indoor temperature set point. The electricity saving ratio reached to a maximum value of 50.8% by using PCM based TES system as compared to a base case. While it was increased to 33.6% as compared to conventional night ventilation system. Matti et al. [25] optimized the geometries of polyethylene encapsulated PCM plates for energy storage applications by experimental as well as numerical work. After simulating 217 different geometries, they came up with optimized ones which can provide increased thermo–hydraulic efficiency up to 50%. In another work, Dardir et al. [10] constructed two PCM-air heat exchangers to enhance the radiation heat transfer during the solidification process of the PCM storage. The systems were tested for cooling of the PCM by exposing it to night sky. They concluded that the ambient air temperature and the condition of the sky during the solidification process were the most important factors. The solidification rate was increased 22% when the system was open to clear night sky. Sun et al. [26] did experimental work to investigate the effect of inclination angle of rectangular PCM slabs (placed horizontally inside a wind tunnel), air temperature and air velocity on melting rate and energy charging speed of the PCM. The melting rate was enhanced by increasing the air velocity. Energy charging speed increased at higher inlet air temperature and at an inclination angle of 90°. A special type of indirect evaporative and storage cooling unit was optimized through simulations by Jaber and Ajib [27] for a residential building. The model could provide 80% cooling energy saving for the specified application with a payback time of 7.8 years. Nie et al. [28] modelled a PCM-based thermal energy storage system aiming to increase the heat transfer rate from the system by applying several design configurations based on application of fins. They found almost 85% decrease in charging time and 74% in discharging time for the PCM. A laboratory scale TES system was manufactured and tested to validate the numerical model. The TES system when integrated with an air-conditioning system, provided stability in the outlet temperature of the air-conditioning system. Amin et al. [29] performed numerical study on PCM encapsulated in plates and introduced a new parameter called energy storage effectiveness to optimize the design of PCM thermal energy storage systems. Mosaffa et al. [30] numerically investigated the effect of air gap size between the PCM slabs and length and thickness of PCM slabs on the performance of a multi-PCM thermal energy storage system. They concluded that the optimum design of the TES system, which was capable of providing desired comfort conditions, consisted of one organic and one inorganic PCM and had a Coefficient of Performance (COP) of 7.0. In another experimental work, Labat et al. [31] tested a PCM based thermal energy storage at multiple air flow rates to store 1 kW of thermal power in 2 h. The results showed that the achieved heating power was less than the target value in two hours but was sufficient enough to be used for validating their numerical model. Darzi et al. [32] numerically optimized plate type heat exchanger equipped with PCM based energy storage at different flow rates. They found out that the melting rates were increased at higher mass flow rates and had a linear relation with thickness of the PCM plates. Nekoonam and Ghasempour [33] developed 2-D concentric dispersion numerical model using apparent heat capacity method to investigate performance of thermal energy storage integrated with solar system. A Generic Algorithm with a novel approach was employed to improve the performance of PCM. Results showed a significant increase in the performance of the PCM in terms of charging and discharging of the PCM and the energy stored by the PCM.

There are only a few research works, as per the authors' knowledge, which have investigated the methods to reduce the pressure loss through PCM based TES systems as well as improve flow non-uniformity in stand-alone PCM storage designs. In one of the studies, Osterman et al. [34] performed experimental work on a TES system consisting of 30 PCM plates at different flow rates to investigate the air velocity distribution in the gaps between PCM plates, pressure drop across the unit and thermal performance of the system. Two configurations were tested i) single stack of 30 plates arranged vertically with air gap of 8 mm ii) two stacks of 30 plates in total arranged horizontally with air gap of 10 mm between the plates. A perforated plate was also placed in front of the stack to attain uniform flow distribution. They concluded that uniform flow was achieved by using perforated plate. The thermal energy power was increased from 125 W to 220 W by doubling the mass flow rate of air. They also proposed that the rate of phase change for heating and cooling cycles could be increased by reducing the thickness of the PCM plates from 15 mm to 10 mm.

The study presented in this paper investigates the performance of PCM based TES system for building cooling applications. The work is a step forward from previous studies as this system has been investigated as a first design of a potential product (in the form of a compact TES system) which will be integrated with a commercially available ventilation system VEX308 [35] to provide a PCM based air cooling module with it for indoor space cooling. The VEX308, in its present form, does not have any facility to cool down the air. The application of such product would not be limited only to ventilation systems but can be extended to small air-conditioning units as well to improve the electrical energy efficiency of the compressor units. The current design also includes a novel wedge-shaped inlet and outlet pressure chambers design for air flow pressure drop compensation in the TES system. An important part of the research done in present work is to experimentally investigate the pressure drop through the PCM storage stacks as well as for the whole TES system for very small air gaps (1.5 mm and 3 mm) between the PCM plates. In most of the cases, this type of PCM storage will eventually be integrated with an HVAC system to achieve comfort conditions. Therefore, pressure drop study through the PCM based TES system is very important in order to ensure that the final design of the energy storage has a pressure drop within the working range of the HVAC system to which it will be integrated. Larger air gaps between PCM plates allow more air to pass through the PCM storage with less pressure drop and less heat transfer. Narrow channels provide faster heat transfer rates and more room for extra PCM plates to be placed within same volume of the system casing (increasing the ratio of plate surface area to total volume) which increases the energy storage potential of the TES system. On the other hand, narrow channels cause bigger pressure drops. Therefore, optimum air channel height is very important to achieve faster charging and discharging rates of the PCM storage by working within the allowable limits of intake pressure for the HVAC system.

In present study, the pressure drop at the outlet of the TES system should be less than 180 *Pa* as a pressure drop more than 180 Pa will reduce the performance of the ventilation system VEX308. Therefore, investigation on the advantage of using a wedge shaped inlet chamber (pressure chamber 1) for the flow to enter uniformly into the gaps between the plates containing

PCM from top to bottom of the PCM stack has been performed. The main objectives of the research work are to investigate the pressure loss across the whole unit, melting and solidification rates of PCM storage at two different air flow rates, and compare the effect of air gap between the plates to increase the potential of the TES system for maximum energy storage and minimum pressure loss.

2. Materials and methods

2.1. The stand-alone TES system

An overview of the thermal energy system is given in Fig. 2. The energy storage system consisted of an aluminum casing with a height of 1036 mm, width 508 mm and length 456 mm. The casing of the system was insulated using 50 mm thick insulation from all sides in order to minimize any heat loss to the environment. It had a single air inlet at the top and single outlet at the bottom on the left side. The PCM rack had an angle of 81.5° with the top surface of the system. The PCM, encapsulated in standard Compact Storage Module (CSM) plates, was provided by Rubitherm Technologies GmbH. The dimensions of each CSM plate were 450 mm × 300 mm × 15 mm. Each plate was filled with a net weight of 2 kg of an inorganic PCM from the manufacturer. Smaller gap size between CSM plates would increase PCM storage density as well as would result in faster melting and solidification rates of the PCM but it would also cause higher pressure loss in the TES system. Due to the restriction of maximum pressure loss through the TES system, two design configurations of the PCM storage were tested, one with smaller gap size and one with relatively bigger gap size between the CSM plates. The CSM plates were arranged in two configurations in the energy storage system: i) 55 CSM plates placed horizontally in a single vertical stack with an air gap of 1.5 mm between the plates and ii) 50 CSM plates placed horizontally in a single vertical stack with an air gap of 3 mm between the plates. The total volume of the casing was constant i.e., same casing of the system was used to place both racks having 1.5 mm gap and 3 mm gap between the plates. The inlet area (pressure chamber1) has a wedge-shaped design to ensure an even pressure distribution from top to bottom at the inlet to the gaps between all the CSM plates. The parameters investigated were air flow pressure loss through the whole unit as a pressure loss of magnitude more than 180 Pa would not be suitable for a successful integration of the TES system with ventilation system VEX308, temperature distribution from top to bottom in the gaps which is very important in order to get maximum potential of the PCM in the stack, and the effect of gap size between CSM plates on melting and solidification rates of the PCM for the two design configurations. A block diagram showing whole research work procedure is given in Fig. 1.

2.2. Phase change material

The phase change material used in this experimental study was inorganic PCM SP21EK produced and supplied by Rubitherm Technologies GmbH. According to the literature supplied by the manufacturer, the SP series of inorganic PCMs have the advantage of showing high thermal energy storage capacity per unit volume, stability throughout the phase change cycles, undergo little supercooling, low flammability, etc. Important thermo-physical properties of SP21EK are presented in Table 1.

3. Experimental setup

Experimental testing was carried out in the Air Handling Unit Laboratory at the Danish Technological Institute. The Lab has test

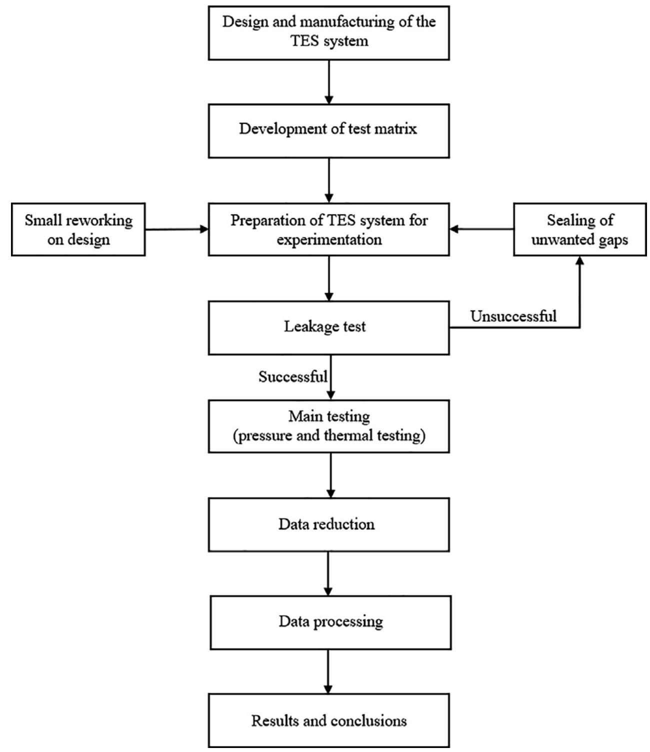

Fig. 1. Block diagram presenting experimental investigation's flow.

facilities which enable the testing of the efficiency, performance and sound power level of residential ventilation units and air handling units. Before the main testing of the system started, any unwanted air gaps on both sides of the CSM plates mounted in the rack were sealed. Also, the air gap at the top and bottom of the PCM rack were sealed in order to avoid any passage of air from any gap which would not produce any heat transfer. The tests carried out were external static pressure test, internal static pressure test and thermal performance testing of the PCM storage. All tests were done in the same test rig with the same duct set up but with different sensors installed or used. The test object was placed in the center of the laboratory as seen in Fig. 3. One "measuring duct" was mounted vertical on the inlet transition duct and one horizontal on the outlet transition duct. Both measuring ducts installed temperature and pressure measurement sensors. The inlet duct was connected to the permanently mounted laboratory test system and the outlet duct was connected to a damper and auxiliary fan.

3.1. Instruments and sensors

External static pressure for the whole unit was measured with pressure instruments of ABB Type 265 DS. The instruments were used for measuring the external pressure in the inlet and outlet and for air flow measurements. Four small boxes were connected to each other with plastic tubes. The ring was then connected to the ABB pressure transmitter. Internal static pressure in each pressure chamber was measured using a pressure sensor SDP810-125 Pa. Ten small boxes were equally divided vertically inside the rack on the inlet and outlet side (sensor 1 near the top of the system and sensor 10 near the bottom of the system), with each box connected to a pressure sensor. Internal and external temperatures were measured using temperature sensors: Type T Cu-CuNi, thermocouples. Same sensors and data acquisition system were calibrated together before the tests were carried out. The sensors were used to measure the internal air temperature in the gap

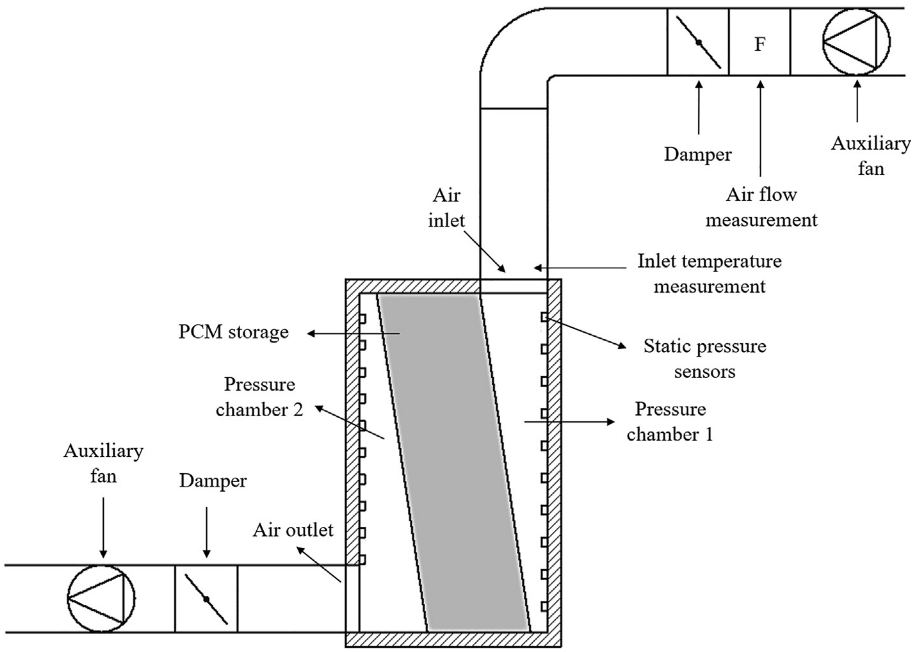

Fig. 2. Schematic diagram of the experimental setup [37].

Table 1
Properties of SP21EK PCM [36].

Properties	Values
Melting temperature range	22–23 °C
Solidification temperature range	21–19 °C
Heat storage capacity (both latent and sensible combined between 13 °C to 28 °C)	170 kJ/kg ± 7.5
Latent heat of fusion	140 kJ/kg
Thermal conductivity	0.5 W/m.K
Specific heat capacity	2 kJ/kg.K
Density in solid phase at 15 °C	1.5 kg/l
Density in liquid phase at 36 °C	1.4 kg/l
Volume expansion	3 to 4%
Maximum operating temperature	45 °C

between the PCM modules and the surface temperature on the PCM modules. The air flow rate was measured with elliptic nozzles in chamber in accordance to ISO5801 on the inlet side. Difference in pressure over the nozzles was measured. The air flow rate was calculated based on equations from ISO5801. For data collection, two different programs were used and the data was transferred to and conditioned in Microsoft Excel software. Table 2 gives an overview of the two of software packages with their application in the data collection. The uncertainty values in pressure measurements and air flow measurements were found to be ±0.5% and ±2%. The uncertainty in temperature measurements was found to be ±0.15 °C.

4. Experimental procedure

4.1. Test conditions

The overall pressure loss test for the TES system was performed at eight different flow rates ranging from 100 m^3/h to 800 m^3/h. For the internal static pressure testing and thermal testing, the flow rates for both 1.5 mm gap size and 3 mm gap size configurations were 400 and 800 m^3/h. The purpose of using same flow rates for both configurations was to analyze the effect of gap size on pressure drop and heat transfer rate by keeping the flow rate constant. During the discharging/melting cycle of the PCM, the temperature of incoming air was kept constant at 27 °C at both flow rates while the initial temperature of the PCM was 13 °C. During the charging/solidification cycle of the PCM, the temperature of incoming air was kept constant at 13 °C at both flow rates while the initial temperature of the PCM was 27 °C.

Fig. 3. Overview of testing arrangement in the lab.

Table 2
Data collection plan.

Measurement	Software	Sampling rate [s]	Average values for [s]
External pressure	Lab View	20	120
Internal pressure	Developed by DTI in Python	1	60
Temperature	Lab View - TI-DOP	1	60
Pressure for flow measurement	Lab View	20	120
Others	Lab View	20	120

4.2. Measured parameters

Internal static pressure measurements were done in the pressure chamber 1 (inlet chamber) and pressure chamber 2 (outlet chamber). For measuring the static pressure, 10 pressure sensors were installed on the inner walls of each pressure chamber at different locations from top to bottom as shown in Fig. 2. The purpose of installing pressure sensors in vertical direction was to investigate uniformity in pressure distribution from top to bottom in the pressure chambers. Even pressure distribution within each pressure chamber would ensure even distribution of airflow from top to bottom in the energy storage. The temperature of the air was measured at the inlet and outlet ducts connected to the system in order to investigate the total heat transfer rate from PCM energy storage which is very important for estimating the efficiency of the storage. The temperature in the second pressure chamber was measured close to the gaps between the CSM plates at 5 different locations as shown in Fig. 4. Eleven temperature sensors in total were used (3 each in gap 1, gap 2 and gap 3 and 1 each in gap 2 and gap 4). This is done to investigate the uniformity in the distribution of heat from top to bottom within the energy storage. Although the gap size is same between all the plates, flow distribution from top to bottom in the TES system could be different which can affect the heat transfer rate from PCM at different locations. Surface temperature of CSM plates was measured for three different plates installed at three different locations withing the energy storage: one at top location, one at middle of the stack and last one near the bottom of the stack. Six temperature sensors were installed on each plate (three at top surface and three at bottom surface at same points) as shown in Fig. 5. The purpose of this type of measurement is to track the PCM melting front during heating cycle for both design configurations.

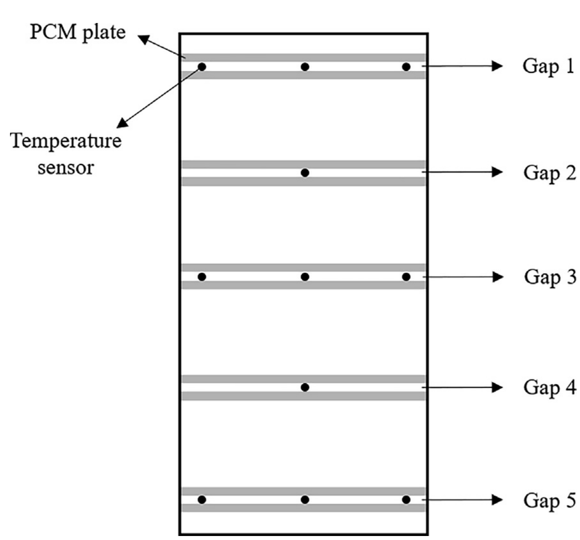

Fig. 4. Positioning of the temperature measurement sensors in pressure chamber 2.

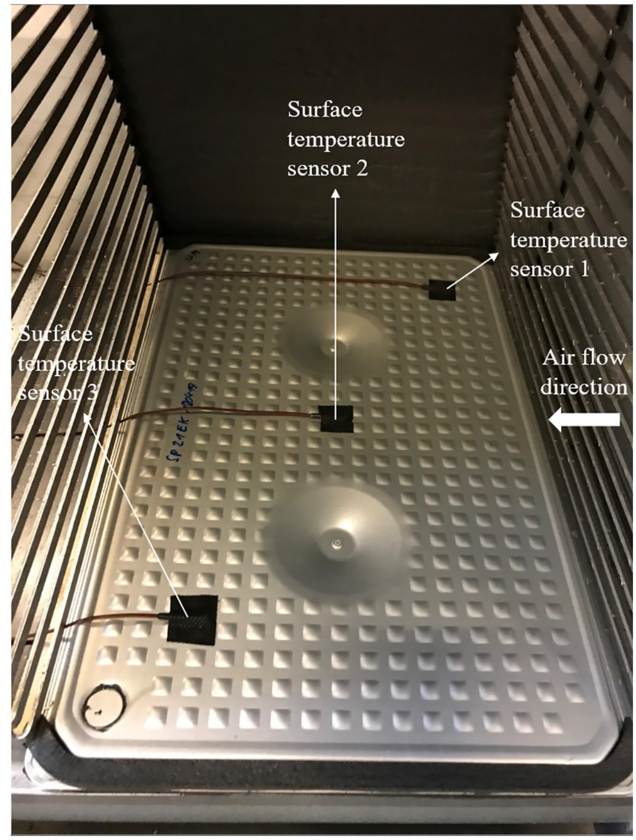

Fig. 5. Positioning of surface temperature measurement sensors on top surface of the CSM plate.

4.3. Running the test

Before performing the main test for the system, preliminary leakage and external pressure loss tests were performed at different air flow rates in order to make sure that there is no leakage of air from the system during the main test. After the leakage test and external pressure loss tests, main testing comprising of static pressure measurements and temperature measurements were done at two air flow rates i.e. 400 m^3/h and 800 m^3/h with one complete heating and solidification cycle for each flow rate for both 1.5 mm and 3 mm system. It was made sure during the tests that the tests should run long enough for the PCM to reach steady state.

5. Analysis

The overall performance of the TES system for both the designs was evaluated by two main parameters at both flow rates: 1) air flow pressure loss during the flow through the system and 2) thermal energy absorbed by the PCM during the discharging/melting process. As explained earlier, the concept of this TES system was developed keeping in view the possibility of integrating the final design with a commercial ventilation system, the maximum pressure drop through the system should be less than 180 Pa for a successful integration with VEX308 ventilation system.

The maximum theoretical heat absorbing potential of the PCM storage was estimated using its sensible heat storage capacity and latent heat storage capacity as:

$$Q_{PCM,th} = Q_{PCM,\mathrm{sensible}} + Q_{PCM,\mathrm{latent}} \quad (1)$$

or

$$Q_{PCM,th} = m_{PCM} C_{p,PCM} (T_{\mathrm{initial}} - T_{\mathrm{final}}) + m_{PCM} h \quad (2)$$

where m_{PCM} is the total mass of the PCM (110 kg for the case of 1.5 mm gap system and 100 kg for the case of 3 mm gap system), $C_{p,PCM}$ is the specific heat capacity of the PCM material, T_{initial} and T_{final} are the initial and final temperatures of the PCM respectively and h is the latent heat of fusion of the PCM.

In order to estimate the amount of thermal energy absorbed by the PCM during the discharging process, an energy balance was applied on the TES system assuming that the energy released/lost by the air passing through the PCM storage was absorbed by the PCM, the mass of the TES system other than the PCM i.e. mass of the inner casing and the stack and energy lost to the environment. The final form of the energy balance is given in Eq. 3

$$Q_{\text{gain,PCM}} = \int_0^t \dot{m}_{\text{air}} C_{p,\text{air}} (T_{\text{air,in}} - T_{\text{air,out}}) dt - Q_{\text{system}} - Q_{\text{envir.}} \tag{3}$$

where $Q_{\text{gain,PCM}}$ is the amount of energy absorbed by the PCM, Q_{system} is the amount of energy absorbed by the material of the system other than the PCM, Q_{envir} is the energy lost to the environment and t is the total time. The expression for heat lost by the air in Eq. 3 was calculated using the relation from the work of [16]. The energy lost by the air with time was calculated in the first term on the right hand side of Eq. 3 in terms of its mass flow rate $\dot{m}_{air}$, specific heat capacity $C_{p,\text{air}}$, inlet temperature $T_{\text{air,in}}$ and outlet temperature $T_{\text{air,out}}$ (measured in the inlet and outlet ducts).

The amount of energy absorbed by casing and rack can be estimated using following equations

$$Q_{\text{system}} = Q_{\text{casing}} + Q_{\text{rack}} \tag{4}$$

$$Q_{\text{casing}} = m_{\text{casing}} C_{p,\text{casing}} (T_{\text{initial}} - T_{\text{final}}) \tag{5}$$

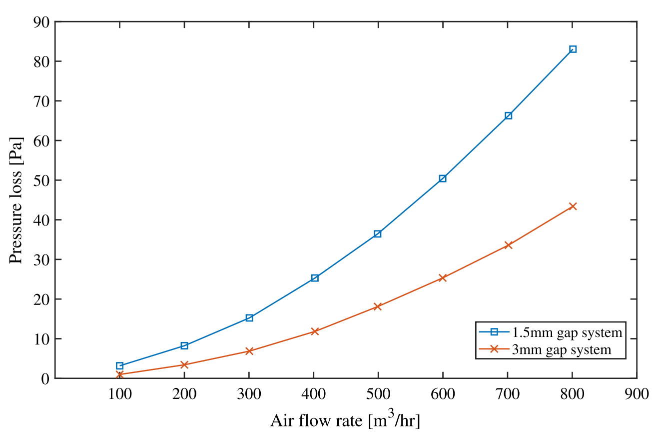

Fig. 6. Overall pressure loss through 1.5 mm and 3 mm gap systems.

$$Q_{\text{rack}} = m_{\text{rack}} C_{p,\text{rack}} (T_{\text{initial}} - T_{\text{final}}) \tag{6}$$

where m_{casing} and m_{rack} are the respective masses of the casing and rack materials, $C_{p,\text{casing}}$ and $C_{p,\text{rack}}$ are the specific heat capacities of the casing and rack materials respectively, $T_{initial}$ and T_{final} are the initial and final temperatures of the system components respectively. After the PCM reached thermal equilibrium with incoming air, any changes in the outlet air temperature of the system correspond to heat losses to the environment. Since the experiments were run for considerably longer periods of time and steady state conditions were comfortably reached, the data of the last one hour of the experiments was used to estimate the average heat loss to the environment by using the relation given in the first term on the right hand side of the Eq. 3.

In order to find the utilization of the PCM potential by the two systems, a parameter called "System efficiency" was introduced in Eq. 7

$$\text{Systemefficiency} = \frac{Q_{\text{gain},PCM}}{Q_{PCM,th}} \times 100 \tag{7}$$

6. Results and discussion

6.1. Pressure test results

At first, a leakage test of the empty system was performed. The rack used to place PCM plates was removed from the casing. The test was done at three flow rates 100, 250 and 400 m^3/h. The difference in the pressure values at the inlet and outlet of the system was negligibly small (approximately 1 Pa) at all the three flow rates which indicated that there was no leakage in the system during the air flow operation.

The overall static pressure loss test was done at eight different flow rates from 100 m^3/h to 800 m^3/h for both 1.5 mm and 3 mm gap systems. The measurements were taken in the inlet and outlet ducts connected to the inlet and outlet of the systems. Fig. 6 shows the results obtained from the overall static pressure loss test for both 1.5 mm and 3 mm systems. From the figure, it can be observed that the maximum pressure drops for both 1.5 mm and 3 mm systems occur at 800 m^3/h, i.e. 83 Pa and 43.3 Pa respectively, which is well within the allowable limits described above.

The static pressure inside the system was measured at 10 locations from top to bottom in both pressure chambers for both 1.5 mm and 3 mm systems at flow rates of 400 and 800 m^3/h. The results of the test have been presented in Table 3 and 4. The static pressure measurements were done using the pressure sensor SDP810-125 Pa which has the tolerance of ±2 Pa. Standard deviation was calculated for the obtained values in each pressure chamber (except for sensor 1 in first chamber and sensors 9 and 10 in

Table 3
Static pressure distribution in pressure chambers 1 and 2 for 1.5 mm system at 400 and 800 m^3/h.

Sensor position	1.5 mm system at 400 m^3/h		1.5 mm system at 800 m^3/h	
	Pressure chamber 1 [Pa]	Pressure chamber 2 [Pa]	Pressure chamber 1 [Pa]	Pressure chamber 2 [Pa]
1	59.69	38.66	87.00	30.82
2	57.83	39.70	86.81	30.72
3	56.27	39.86	81.57	31.55
4	58.25	42.10	89.38	31.84
5	56.47	40.87	86.57	31.75
6	57.89	42.21	81.08	31.53
7	57.73	40.07	86.69	30.70
8	58.70	41.38	85.09	30.14
9	56.71	39.48	87.36	25.95
10	56.98	40.81	85.45	23.31
Standard deviation	0.85	1.10	2.69	0.62

Table 4
Static pressure distribution in pressure chambers 1 and 2 for 3 mm system at 400 and 800 m^3/h.

Sensor position	3 mm system at 400 m^3/h		3 mm system at 800 m^3/h	
	Pressure chamber 1 [Pa]	Pressure chamber 2 [Pa]	Pressure chamber 1 [Pa]	Pressure chamber 2 [Pa]
1	105.97	91.14	112.46	90.60
2	100.11	95.93	108.39	91.48
3	99.62	92.83	107.20	90.41
4	101.18	97.05	108.97	92.11
5	100.41	93.78	107.29	90.95
6	101.08	96.93	109.19	91.32
7	101.93	94.38	108.90	87.97
8	101.22	93.97	109.80	87.69
9	97.05	91.57	106.34	83.15
10	100.66	92.53	108.62	81.84
Standard deviation	1.42	1.99	1.12	1.62

the second chamber because they were placed near the inlet and outlet of the system and experience larger pressure changes). It was observed from the results that the standard deviation of the pressure values for the case of each pressure chamber was within the tolerance limits of the sensors. Which suggests that there is no significant difference in the values obtained from the pressure sensors in each chamber. Based on this observation, it can be said that the pressure distribution in each pressure chamber for both the systems at both flow rates was relatively uniform from top to bottom.

6.2. Thermal performance analysis during heating and cooling of the PCM

6.2.1. PCM discharging/melting cycle

Testing for discharging cycle of both systems was done at a constant inlet air temperature of 27 °C at flow rates of 400 m^3/h and 800 m^3/h. The PCM plates were kept at a constant temperature of 13 °C before the start of the heating cycle. In order to investigate the uniformity in the temperature distribution from top to bottom for the energy storage system, temperature sensors were installed at 5 locations from top to bottom in the second pressure chamber to measure the air temperature coming out of the gaps between the PCM plates (see Fig. 4). As there were three sensors each in gap 1, 3 and 5, average values for the three sensors in these gaps were taken for the purpose of comparison.

A comparison of 1.5 mm and 3 mm systems has been given in Fig. 7 at a flow rate of 400 m^3/h. For 1.5 mm system, the temperature distribution from gap 1 to 4 was relatively uniform. But for the case of gap 5, located near the bottom of the system, the PCM did not reach to the same temperature as other regions in the storage did. This suggests that the material of the system other than the PCM, also stored heat in the sensible form as the air moved from top to bottom in pressure chamber 1. For the 3 mm system, the temperature distribution from gap 2 to gap 4 was relatively uniform. A lower temperature was achieved in the region where gap 1 was located (top gap). A possible reason for this could be the presence of bigger gaps between the plates which resulted in faster downward motion of flow. As a results, air mass flow rate through the gaps was low in the top area of the system and heat transfer rate there was lower than in other regions. For the case of the bottom gap (gap 5), similar results were shown as for the 1.5 mm system, i.e. less heat reaching to the bottom of the storage because of heat absorption by the material of the casing and PCM storage as air flows from top to bottom in pressure chamber 1.

The results of heating cycle at 800 m^3/h for both gap systems are shown in Fig. 8. In terms of temperature distribution, same kind of results were observed for both 1.5 mm and 3 mm systems. This is because the airflow paths from inlet to outlet were same for both design configurations. The only noticeable difference was the effect of flow rate on the complete melting of the PCM storage. As the flow rate was increased from 400 m^3/h to 800 m^3/h, the heat absorption from incoming air to the PCM was also increased which resulted in faster melting rate of the PCM storage.

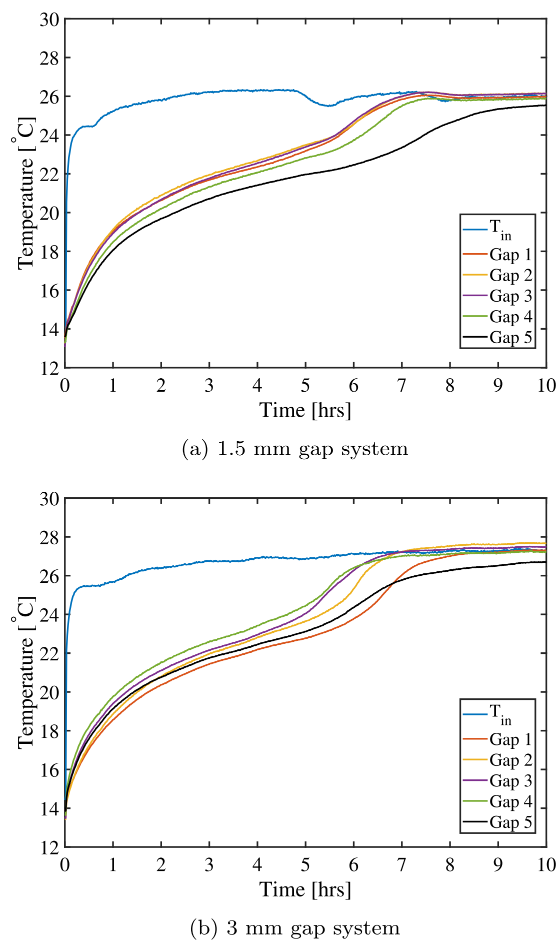

Fig. 7. Temperature distribution in the system from top to bottom of PCM stack; melting at 400 m^3/h for (a) 1.5 mm gap system (b) 3 mm gap system.

6.2.2. Cooling/solidification cycle

The solidification or charging cycle of the PCM storage for both designs was performed at a constant air inlet temperature of 13 °C at 400 and 800 m^3/h flow rates. Before the start of the process,

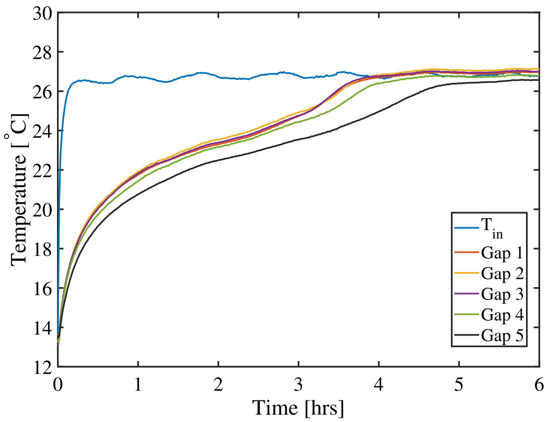

(a) 1.5 mm gap system

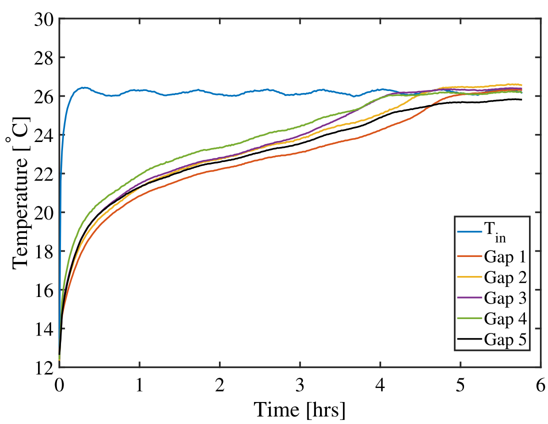

(b) 3 mm gap system

Fig. 8. Temperature distribution in the system from top to bottom of PCM stack; melting at 800 m^3/h for (a) 1.5 mm gap system (b) 3 mm gap system.

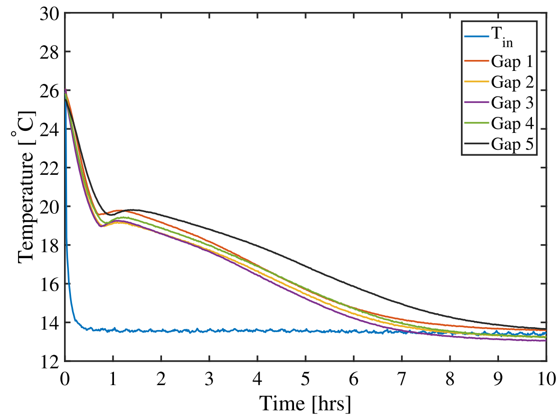

(a) 1.5 mm gap system

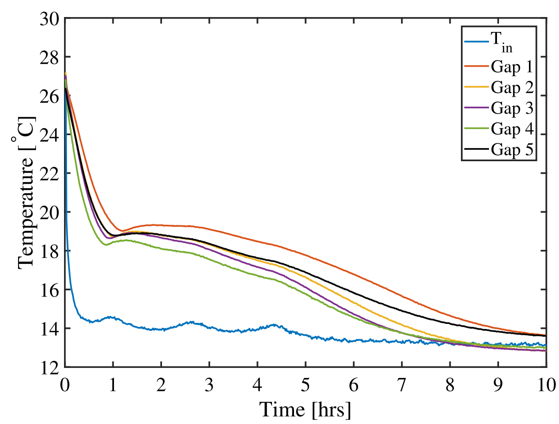

(b) 3 mm gap system

Fig. 9. Temperature distribution in the system from top to bottom of PCM stack; solidification at 400 m^3/h for (a) 1.5 mm gap system (b) 3 mm gap system.

PCM plates were kept at 27 °C to make sure that the PCM inside the plates was in completely melted form. The results for the solidification cycle at both flow rates are shown in Figs. 9 and 10. The trend of the temperature distribution from top to bottom in all the five gaps was same as was seen for the case of the melting cycle. A slightly higher heat transfer rate in the case of 3 mm system was observed for the region of gap 4 which lies in lower middle part of the PCM stack. Due to the presence of the outlet on the left side of the system and bigger gaps between the plates in 3 mm gap system, the flow was faster in this region of the storage than the other regions of the PCM storage which results in a higher heat transfer rate. On the other hand, flow was more uniformly distributed from top to bottom for most of the PCM storage in the case of 1.5 mm system.

6.2.3. PCM melting front

In order to investigate the melting of the PCM within the CSM plate, six thermocouple sensors were installed on the upper and lower surfaces of three different plates. For each CSM plate, three thermocouples were installed on the upper surface (see Fig. 5) and three at the bottom surface exactly below the same points, where the sensors were installed on the upper surface. The sensors were placed such that the plates were divided into three regions: first region near the leading edge of the plate (location 1), middle region (location 2) and last region (location 3). These three plates with surface temperature measurement sensors were placed in the top (Plate 1), middle (Plate 2) and bottom (Plate 3) sections of the PCM storage. All three plates were kept at 13 °C, which was well below the solidification temperature of the PCM (21–19 °C) before the start of melting cycle to ensure that the PCM was completely solid. When air at 27 °C comes in contact with the PCM plates, heat transfer takes place from air to the PCM and continues until both PCM and air reach thermal equilibrium. It is expected that the heat transfer between the air and the PCM in the region where it comes into contact first, location 1, is faster than the other two locations. Or it can be expressed in terms of PCM temperatures as: $T_1 > T_2 > T_3$.

For the purpose of illustration, only the results of PCM melting cycle at flow rate of 400 m^3/h for both gap systems are shown in Figs. 11 and 12. For the 1.5 mm gap system (Fig. 11), it was observed that the PCM melting front moved smoothly from location 1 to location 3 throughout the melting process for all the three plates. The heat transfer rate between air and the PCM was fastest near the leading edge of the plates (location 1). As the air moved along the plates, its temperature was lowered and due to this reason, the middle and the last portions of the plates received lesser heat and they melt at a lower rate. As soon as the thermal equilibrium was achieved between the melted PCM and air, heat transfer between the air and CSM plates stopped. For the 3 mm gap system (Fig. 12), temperatures achieved for first and middle regions of plate 1 were almost same for a period of approximately 3.5 h but remain higher than the last region until the PCM was completely melted. Whereas for plate 2 and plate 3, heat transfer rate in the first region of the plate was faster than the middle and last regions.

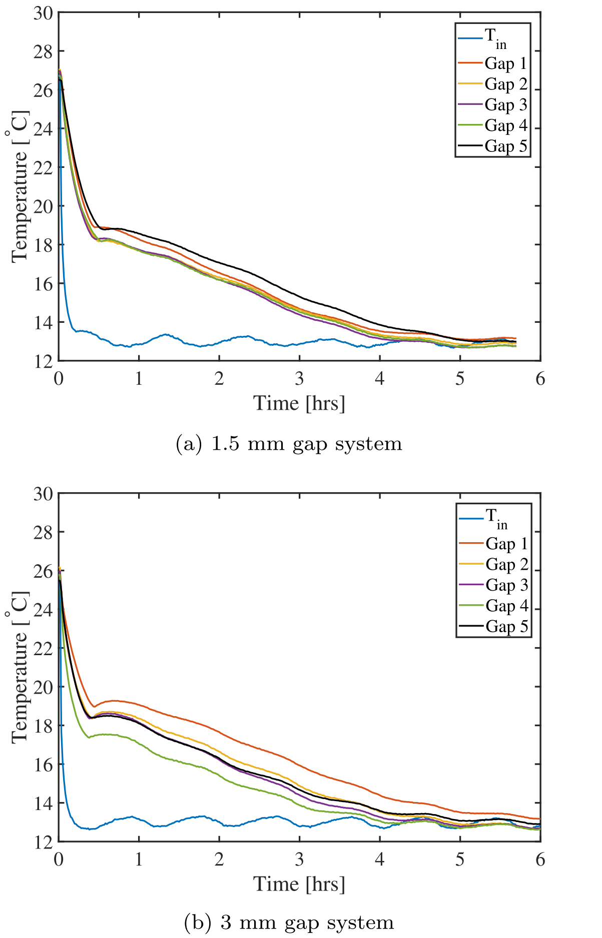

(a) 1.5 mm gap system

(b) 3 mm gap system

Fig. 10. Temperature distribution in the system from top to bottom of PCM stack; solidification at 800 m^3/h for (a) 1.5 mm gap system (b) 3 mm gap system.

For the same plates, in middle and last regions, heat transfer rates were almost same for a period of first 1.7 h and then middle region melted faster than the last region.

It was noted for both 1.5 mm and 3 mm gap systems that the temperature of the PCM in the bottom plate (plate 3) did not reach to the inlet air temperature of the air,i.e. 27 °C (measured in the inlet duct), even after 10 h of heating. This was because the air temperature became less than 27 °C when it reached the bottom part of the PCM storage, because of the heat transfer to the casing of the system and PCM during the movement of air from inlet to the bottom part of the PCM storage.

6.2.4. PCM discharging and charging time

As described earlier, both the energy storage systems with 1.5 mm and 3 mm gap size between the CSM plates were tested at two flow rates, i.e., 400 m^3/h and 800 m^3/h. The increase in the gap size between the plates, as well as the increase in the flow velocity of the air, affect the rate of heat transfer between the air and PCM. Table 5 shows the times taken by both the systems to reach steady state at the two flow rates. During the discharging process, the 1.5 mm system reached to steady state one hour faster at 400 m^3/h and half an hour faster at 800 m^3/h than the 3 mm system. Same kind of results were observed when the two systems are compared for the charging process at 400 m^3/h and 800 m^3/h. This happened because the air velocity in the 1.5 mm channel is higher compared to the 3 mm channel resulting in higher heat transfer rate than the 3 mm gap system.

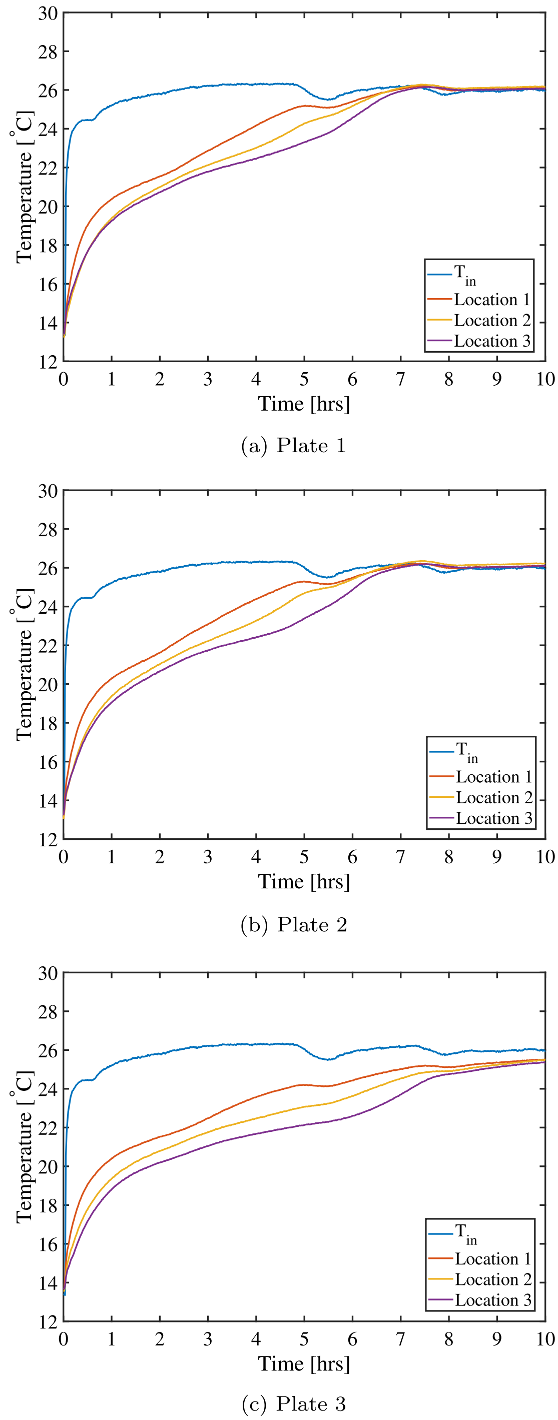

(a) Plate 1

(b) Plate 2

(c) Plate 3

Fig. 11. Temperature distribution inside the CSM plate; PCM melting at 400 m^3/h for 1.5 mm system.

When the flow rate is doubled from 400 m^3/h to 800 m^3/h, the time taken by the PCM in both 1.5 mm and 3 mm systems reduced significantly to reach steady state during discharging and charging processes. The time taken by both 1.5 mm and 3 mm systems to reach steady state during the discharging process is decreased by almost 40% and 41.2% respectively, by increasing the flow rate from 400 m^3/h to 800 m^3/h. During the charging process, the time taken to reach steady state is reduced by almost 48.3% for 1.5 mm and 47.4% for 3 mm system by increasing the flow rate from 400 m^3/h to 800 m^3/h.

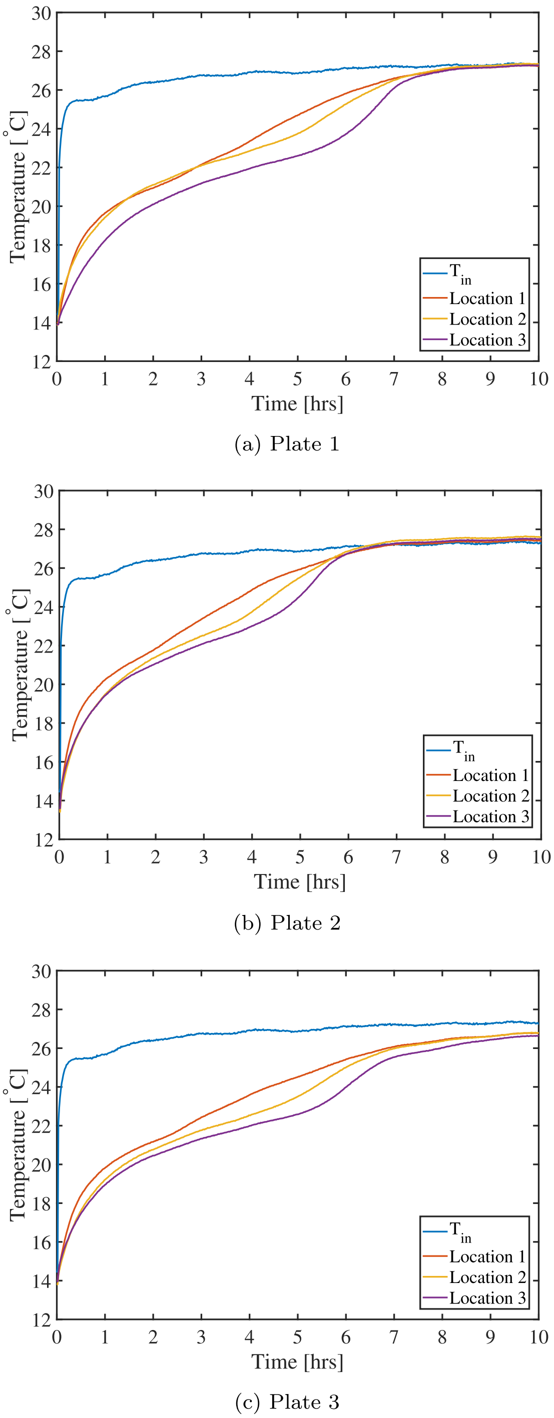

Fig. 12. Temperature distribution inside the CSM plate; PCM melting at 400 m^3/h for 3 mm system.

6.2.5. Thermal energy stored

The purpose of using a PCM storage with a ventilation system is to provide the already stored "cold" (heat released during the solidification process of the PCM) in the PCM storage to lower the temperature of incoming air. During the discharging process of the PCM, when air at higher temperature than the PCM storage was passed through the PCM storage, it lost heat to the storage and subsequently its temperature was lowered.

The maximum theoretical potential of the PCM for both the systems was estimated by using Eqs. 1 and 2 given in Section 5. The amount of thermal energy absorbed by the PCM during the experiment was calculated using Eq. 3 given in Section 5. The losses were estimated according to the methodology described in Section 5 and heat absorbed by other system components was estimated using Eqs. 5 and 6. A comparison of the amount of energy absorbed by the PCM during the discharging process of the PCM is given in Fig. 13 for both 1.5 mm and 3 mm systems at a flow rate of 400 m^3/h. The system efficiency for 1.5 mm and 3 mm systems was calculated using Eq. 7. Both the systems show almost same efficiency by utilizing approximately 78.3% of the available theoretical potential of the PCM. But the 1.5 mm system provides overall more energy storage potential than the 3 mm system. For a charging process of 10 h, the PCM in 1.5 mm system absorbs approximately 14290 *kJ* of heat energy from air which is almost 8.7% more energy storage potential than 3 mm system which absorbs 13150 *kJ*. This extra energy storage potential is because of the presence of 10 kg of more PCM in 1.5 mm system than the 3 mm system in the same casing. The narrow channels in 1.5 mm system allow more space for more PCM plates to be used, hence increasing the energy storage potential.

Cooling the air using PCM based thermal energy storage has been investigated by many researchers using different types of

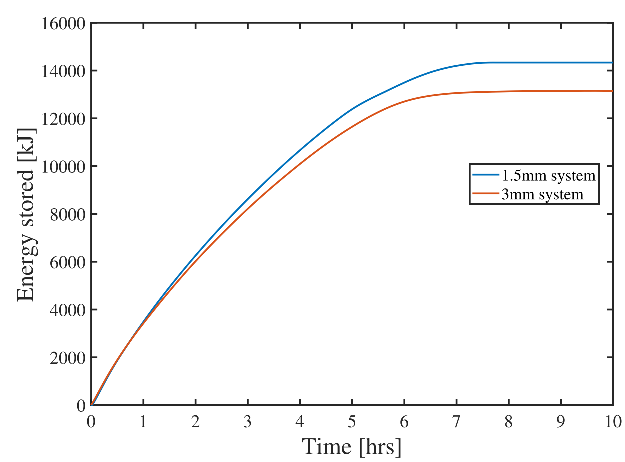

Fig. 13. Comparison of cumulative energy stored by the PCM storage of both the systems during discharging process at 400 m^3/h.

Table 5
PCM discharging and charging times to reach steady state.

Design type	Discharging time at 400 m^3/h [hours]	Charging time at 400 m^3/h [hours]	Discharging time at 800 m^3/h [hours]	Charging time at 800 m^3/h [hours]
1.5 mm system	7.5	8.7	4.5	4.5
3 mm system	8.5	10	5	5

PCM storage designs. In some investigations, researchers have used almost same CSM plates encapsulating the PCM. Zeinelabdein et al. [17] studied the PCM storage performance with two PCM stacks (containing same PCM) placed in series with variable air gaps of 10 mm, 15 mm and 20 mm at different air inlet temperatures and flow rates. Osterman et al. [34] also used PCM CSM plates in vertical arrangement with air gap of 8 mm and in horizontal configuration with air gaps of 10 mm and tested the TES systems at different air flow rates and air inlet temperatures. Kumirai et al. [16] used CSM plates in vertical arrangement with an air gap of 5 mm between the plates and tested the same way as above. They all observed that the PCM melting and solidification rates are positively affected by increasing the inlet air temperature and air flow rates. Narrow air gaps between PCM plates produced faster melting and solidification rates as compared to wider air gaps and increased energy storage density of the PCM storage. Same kind of results were seen in present research work. The 1.5 mm design configuration showed faster melting and solidification results as compared to 3 mm gap size and provided almost 8.7% more energy storage potential than 3 mm system. Also, when the air flow rate was increased from 400 m^3/h to 800 m^3/h, faster PCM melting and solidification results were observed.

7. Conclusions

Two thermal energy storage system design configurations (1.5 mm and 3 mm gap size between PCM CSM plates) were investigated in this research work to study pressure drop in the system, pressure distribution in pressure chambers 1 and 2, temperature distribution within the system and overall energy storage potential of the TES system. This research was done to investigate the first design of the TES system intended to be integrated with commercial ventilation system VEX308. Based on the results for pressure tests, it was concluded that the overall pressure drop for both the configurations was less than 180 *Pa* (maximum pressure drops for both 1.5 mm and 3 mm systems occurred at 800 m^3/h, i.e. 83 Pa and 43.3 Pa respectively), which satisfied the condition for a possible integration of the TES system with a VEX308 ventilation system. Also, the pressure distribution in each pressure chamber from top to bottom was relatively uniform. The concept of wedge-shaped flow region for both pressure chambers was found suitable for providing even pressure distribution in both design configurations. temperature distribution study from top to bottom within the TES systems was done at five different locations after the PCM stack in pressure chamber 2. Results showed that the temperature distribution was relatively fair from top to bottom in the energy storage for both the design configurations at both flow rates. The bottom region of the PCM storage received less heat because of heat loss from incoming air to the casing of the system and also to the PCM storage as it moved from top to bottom in pressure chamber 1. The 1.5 mm gap design for the energy storage system having 55 CSM plates and 110 kg PCM showed faster heating and cooling rates at both the flow rates as compared to the 3 mm system, which had 50 CSM plates and 100 kg PCM. Both the systems showed almost same efficiency (approximately 78.3%) for PCM utilization. The 1.5 mm system provided almost 8.7% more energy storage potential as compared to 3 mm system. This was possible because of the presence of 10 kg of more PCM in 1.5 mm system than 3 mm system. Based on the results from both the design configurations, the 1.5 mm gap configuration was considered more suitable for a possible integration with VEX308 ventilation system.

The experimental study presented in this paper was performed on stand-alone TES system keeping in view its possible integration with commercial ventilation system VEX308. At this moment, the testing on the TES system was done without connecting it with VEX308 ventilation system. So, it is recommended that its performance should be experimentally be tested in real life operation conditions while it is integrated with VEX308 with all ducts and other components connected.

Declaration of Competing Interest

The authors declare that they have no known competing financial interests or personal relationships that could have appeared to influence the work reported in this paper.

Acknowledgements

This work was financed by the NeGeV project which is funded by the Danish Energy Agency under the Energy Technology Development and Demonstration Program (EUDP Project No. 64017–05117). The authors also acknowledge Mads Høi Rasmussen from University of Southern Denmark for his contributions in developing the design of the TES system.

References

[1] D.K. Bhamare, M.K. Rathod, J. Banerjee, Passive cooling techniques for building and their applicability in different climatic zones–the state of art, Energy Build. 198 (2019) 467–490.
[2] R. Zeinelabdein, S. Omer, G. Gan, Critical review of latent heat storage systems for free cooling in buildings, Renew. Sustain. Energy Rev. 82 (2018) 2843–2868.
[3] S. Drissi, T.-C. Ling, K.H. Mo, A. Eddhahak, A review of microencapsulated and composite phase change materials: Alteration of strength and thermal properties of cement-based materials, Renew. Sustain. Energy Rev. 110 (2019) 467–484.
[4] K. Faraj, M. Khaled, J. Faraj, F. Hachem, C. Castelain, Phase change material thermal energy storage systems for cooling applications in buildings: A review, Renew. Sustain. Energy Rev. 119 (2020).
[5] P. Huovila, M. Ala-Juusela, L. Melchert, S. Pouffary, C.-C. Cheng, D. Ürge-Vorsatz, S. Koeppel, N. Svenningsen, P. Graham, Buildings and Climate, Summary for Decision-Makers, United Nations Environment Programme, Change, 2009.
[6] A. Waqas, Z.U. Din, Phase change material (pcm) storage for free cooling of buildings–a review, Renew. Sustain. Energy Rev. 18 (2013) 607–625.
[7] Y. Xuan, F. Xiao, X. Niu, X. Huang, S. Wang, Research and application of evaporative cooling in china: A review (i)–research, Renew. Sustain. Energy Rev. 16 (5) (2012) 3535–3546.
[8] F. Al-Ajmi, D. Loveday, V.I. Hanby, The cooling potential of earth–air heat exchangers for domestic buildings in a desert climate, Build. Environ. 41 (3) (2006) 235–244.
[9] B. Zalba, J.M. Marin, L.F. Cabeza, H. Mehling, Free-cooling of buildings with phase change materials, Int. J. Refrig 27 (8) (2004) 839–849.
[10] M. Dardir, L. Roccamena, M. El Mankibi, F. Haghighat, Performance analysis of an improved pcm-to-air heat exchanger for building envelope applications–an experimental study, Sol. Energy 199 (2020) 704–720.
[11] H. Akeiber, P. Nejat, M.Z.A. Majid, M.A. Wahid, F. Jomehzadeh, I.Z. Famileh, J.K. Calautit, B.R. Hughes, S.A. Zaki, A review on phase change material (pcm) for sustainable passive cooling in building envelopes, Renew. Sustain. Energy Rev. 60 (2016) 1470–1497.
[12] A. Maccarini, G. Hultmark, N.C. Bergsøe, A. Afshari, Free cooling potential of a pcm-based heat exchanger coupled with a novel hvac system for simultaneous heating and cooling of buildings, Sustain. Cities Soc. 42 (2018) 384–395.
[13] S.A. Memon, Phase change materials integrated in building walls: A state of the art review, Renewab. Sustain. Energy Rev. 31 (2014) 870–906.
[14] S.A. Mohamed, F.A. Al-Sulaiman, N.I. Ibrahim, M.H. Zahir, A. Al-Ahmed, R. Saidur, B. Yılbaş, A. Sahin, A review on current status and challenges of inorganic phase change materials for thermal energy storage systems, Renew. Sustain. Energy Rev. 70 (2017) 1072–1089.
[15] A. De Gracia, L.F. Cabeza, Phase change materials and thermal energy storage for buildings, Energy Build. 103 (2015) 414–419.
[16] T. Kumirai, J. Dirker, J. Meyer, Experimental analysis for thermal storage performance of three types of plate encapsulated phase change materials in air heat exchangers for ventilation applications, J. Build. Eng. 22 (2019) 75–89.
[17] R. Zeinelabdein, S. Omer, G. Gan, Experimental performance of latent thermal energy storage for sustainable cooling of buildings in hot-arid regions, Energy Build. 186 (2019) 169–185.
[18] R. Zeinelabdein, S. Omer, E. Mohamed, Parametric study of a sustainable cooling system integrating phase change material energy storage for buildings, J. Energy Storage 32 (2020).
[19] S. Nekoonam, R. Ghasempour, Optimization of a solar cascaded phase change slab-plate heat exchanger thermal storage system, J. Energy Storage 34 (2021).

[20] M. Iten, S. Liu, A. Shukla, Experimental study on the thermal performance of air-pcm unit, Build. Environ. 105 (2016) 128–139.
[21] S. Nada, W. Alshaer, R. Saleh, Experimental investigation of pcm transient performance in free cooling of the fresh air of air conditioning systems, J. Build. Eng. 29 (2020).
[22] S. Nekoonam, R. Roshandel, Modeling and optimization of a multiple (cascading) phase change material solar storage system, Therm. Sci. Eng. Progress 23 (2021).
[23] G. Gholamibozanjani, M. Farid, Application of an active pcm storage system into a building for heating/cooling load reduction, Energy 210 (2020).
[24] X. Chen, Q. Zhang, Z.J. Zhai, X. Ma, Potential of ventilation systems with thermal energy storage using pcms applied to air conditioned buildings, Renewable Energy 138 (2019) 39–53.
[25] M. Grabo, C. Staggenborg, K.A. Philippi, E. Kenig, Modeling and optimization of rectangular latent heat storage elements in an air-guided heat storage system, Front. Energy Res. 8 (2020) 249.
[26] X. Sun, Y. Chu, M.A. Medina, Y. Mo, S. Fan, S. Liao, Experimental investigations on the thermal behavior of phase change material (pcm) in ventilated slabs, Appl. Therm. Eng. 148 (2019) 1359–1369.
[27] S. Jaber, S. Ajib, Novel cooling unit using pcm for residential application, Int. J. Refrig. 35 (5) (2012) 1292–1303.
[28] B. Nie, Z. Du, B. Zou, Y. Li, Y. Ding, Performance enhancement of a phase-change-material based thermal energy storage device for air-conditioning applications, Energy Build. 214 (2020).
[29] N.A.M. Amin, M. Belusko, F. Bruno, M. Liu, Optimising pcm thermal storage systems for maximum energy storage effectiveness, Sol. Energy 86 (9) (2012) 2263–2272.
[30] A. Mosaffa, C.I. Ferreira, F. Talati, M. Rosen, Thermal performance of a multiple pcm thermal storage unit for free cooling, Energy Convers. Manage. 67 (2013) 1–7.
[31] M. Labat, J. Virgone, D. David, F. Kuznik, Experimental assessment of a pcm to air heat exchanger storage system for building ventilation application, Appl. Therm. Eng. 66 (1–2) (2014) 375–382.
[32] A.R. Darzi, S. Moosania, F. Tan, M. Farhadi, Numerical investigation of free-cooling system using plate type pcm storage, Int. Commun. Heat Mass Transfer 48 (2013) 155–163.
[33] S. Nekoonam, R. Ghasempour, Modeling and optimization of a thermal energy storage unit with cascaded pcm capsules in connection to a solar collector, Sustain. Energy Technol. Assess. 52 (2022).
[34] E. Osterman, K. Hagel, C. Rathgeber, V. Butala, U. Stritih, Parametrical analysis of latent heat and cold storage for heating and cooling of rooms, Appl. Therm. Eng. 84 (2015) 138–149.
[35] Exhausto,https://www.exhausto.dk/vex308.
[36] Rubitherm,https://www.rubitherm.eu/en/index.php/productcategory/anorganische-pcm-sp.
[37] M.H. Rasmussen, An apparatus for temperature regulation in a building and a hybrid ventilation system and a method with such apparatus (European Patent Application No. 22150287.5, Unpublished (filing date January 5, 2022)).